Crystal structure of 1-ferrocenyl-2-(4-nitrophenyl)-ethyne

Sara M. Delgado Rivera,[a] Jean C. González Espiet,[b] Jesús M. Dones,[a] Sebastián A. Henríquez López,[a] Ana R. Guadalupe,[a] Dalice M. Piñero Cruz[b] and Ingrid Montes González[a]*

[a]Department of Chemistry, University of Puerto Rico at Río Piedras, PO Box 23346, San Juan, PR 00931-3346, Puerto Rico, and [b]Department of Chemistry and the Molecular Sciences Research Center, University of Puerto Rico-Rio Piedras Campus, PO Box 23346, San Juan, 00931-3346, Puerto Rico. *Correspondence e-mail: ingrid.montes2@upr.edu

The title ferrocene derivative, $[Fe(C_5H_5)_2(C_8NO_2)]$, including an alkyne bonded to a *para*-nitrophenyl substituent, which was synthesized from a copper-free Sonogashira cross-coupling reaction between ethynylferrocene and 4-bromo-1-nitrobenzene, crystallizes in the $P2_1/n$ space group. In the ferrocene unit, the pentadienyl (Cps) rings are in an eclipsed conformation. The angle of rotation between the substituted cyclopentadienyl ring and the *p*-nitrophenyl group is 6.19 (10)°, yielding a quasi-linear extension of the ferrocenyl substitution. Important intermolecular interactions arise from π–π stacking between the Cp rings and the *p*-nitrophenyl, from corners of the Cp rings that are perpendicularly aligned, and between the O atoms from the nitro substituent and carbons at the corners of the Cp rings, propagating along all three crystallographic axes.

1. Chemical context

Recent efforts in the field of medicinal organometallic chemistry have been driven by a high interest in the synthesis of metal ethynyl complexes, particularly because of their biological activity (Görmen *et al.*, 2012). In addition, phenyl-ethyne-derived compounds display active electrochemical properties such as the generation of stable redox forms, regeneration at low potentials and good electrochemical reversibility (Gasser & Metzler-Nolte, 2012). 1-Ferrocenyl-2-(4-nitrophenyl)ethyne has previously been prepared in moderate-to-high yields (52–92%) by applying Sonogashira coupling reactions. However, all of them used 4-iodo-1-nitrobenzene or 4-triflate-1-nitrobenzene and a variety of solvents, catalysts and conditions, under an inert atmosphere. The reaction time varied from 25 min to 4 h (Torres *et al.*, 2002; Shoji *et al.*, 2014; Li *et al.*, 2009; Fu *et al.*, 2008; Coutouli-Argyropoulou *et al.*, 2003). Other approaches involved the use of iodoferrocene and 4-ethynyl-1-nitrobenzene (Kulhánek *et al.*, 2013). Our approach focuses on performing copper-free Sonogashira coupling between ethynylferrocene and 4-bromo-1-nitrobenzene without the need of inert atmosphere protocols and obtaining moderate-to-high yields, by following green chemistry protocols.
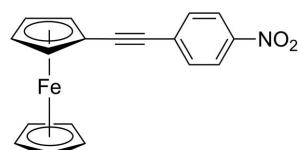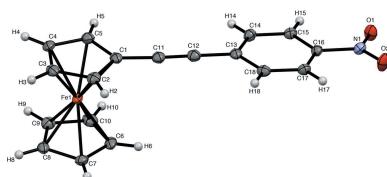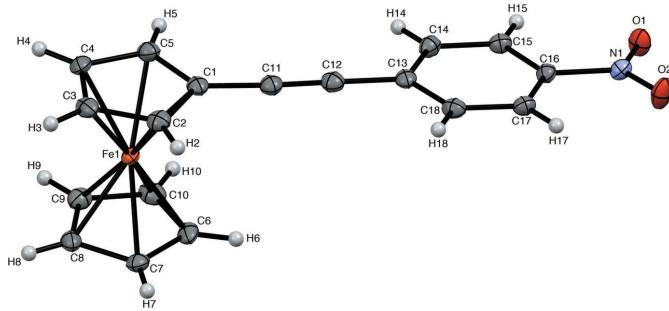
Figure 1
Molecular structure of the title compound, including atom labelling. Displacement ellipsoids are drawn at the 50% probability level.

2. Structural commentary

Fig. 1 (*Mercury*; Macrae *et al.*, 2020) shows the molecular structure of the title compound, which crystallizes in space group $P2_1/n$. The substituted ferrocene (Fc) system is linked to a *p*-nitrobenzene moiety by an acetylenic bridge between C11 and C12 with a bond distance of 1.202 (2) Å, which is comparable to those in similar complexes, *e.g.* 1.202 (2) Å (Misra *et al.* 2014), 1.197 (3) Å (Fu *et al.*, 2008), and 1.193 (2) Å (Zora *et al.* 2006). The unit cell is comprised of four molecules with one molecule present per asymmetric unit. The substituted Cp and phenyl rings are almost parallel to each other, subtending a dihedral angle of 6.19 (10)°, in contrast to (phenyl-ethynyl)ferrocene (Zora *et al.*, 2006), which has no substituent in the *para* position and exhibits a nearly perpendicular dihedral angle of 89.06 (3)°. The distances of the Fe1 atom from the centroids of the substituted and unsubstituted Cp rings are 1.6461 (8) and 1.6584 (8) Å, respectively. The $Cg1$—Fe1—$Cg2$ angle is 179.27°, where $Cg1$ and $Cg2$ are the centroids of substituted and unsubstituted Cp rings, respectively. The Cp rings in the ferrocene system are thus almost parallel, since the angle between the Cp ring

Table 1
Hydrogen-bond geometry (Å, °).

D—H$\cdots A$	D—H	H$\cdots A$	$D\cdots A$	D—H$\cdots A$
C6—H6$\cdots$O1[i]	0.93	2.55	3.461 (2)	168
C15—H15$\cdots$O1[ii]	0.93	2.41	3.1909 (19)	141
C17—H17$\cdots$O2[iii]	0.93	2.49	3.2187 (19)	135

Symmetry codes: (i) $-x, -y+1, -z+1$; (ii) $-x-1, -y+1, -z+1$; (iii) $-x, -y+1, -z$.

planes is 1.03 (13)°. In addition, the Cp rings display a nearly eclipsed conformation with a slight deviation, as demonstrated by the average C—$Cg1$—$Cg2$—C torsion angle of 12.26°. The C—C bond distances in the Cp rings range from 1.417 (2) to 1.436 (2) Å, while the Fe—C bond lengths range between 2.038 (2) and 2.055 (2) Å.

3. Supramolecular features

The title compound exhibits π–π stacking interactions between one of the Cp rings from the Fc moiety and the *p*-nitrophenyl substituent, allowing the formation of a zigzag structure; atom pairs involved relate C6(Cp) and C7(Cp) to C17(*p*-nitrophenyl) and C18(*p*-nitrophenyl) of a neighboring molecule, with short contacts of 3.340 (2) and 3.397 (2) Å, respectively. This interaction can be described as pairs of molecules being interrupted by two C3(Cp)$\cdots$H8—C8(Cp) interactions from a different interconnected pair of perpendicularly oriented Fc moieties with short contact distances of 2.83 Å each. Short contacts from neighboring molecules establishing a distinctive interconnected pair between a corner of the Cp ring and one of the oxygen atoms from the *p*-nitrophenyl substituent yield a closed arrangement of atoms. Short contacts involve H6—C6(Cp)$\cdots$O1(*p*-nitrophenyl) at a distance of 3.461 (2) Å. Another interconnection is found between adjacent *p*-nitrophenyl groups, yielding a ring arrangement involving pairs from H17—C17(*p*-nitrophen-
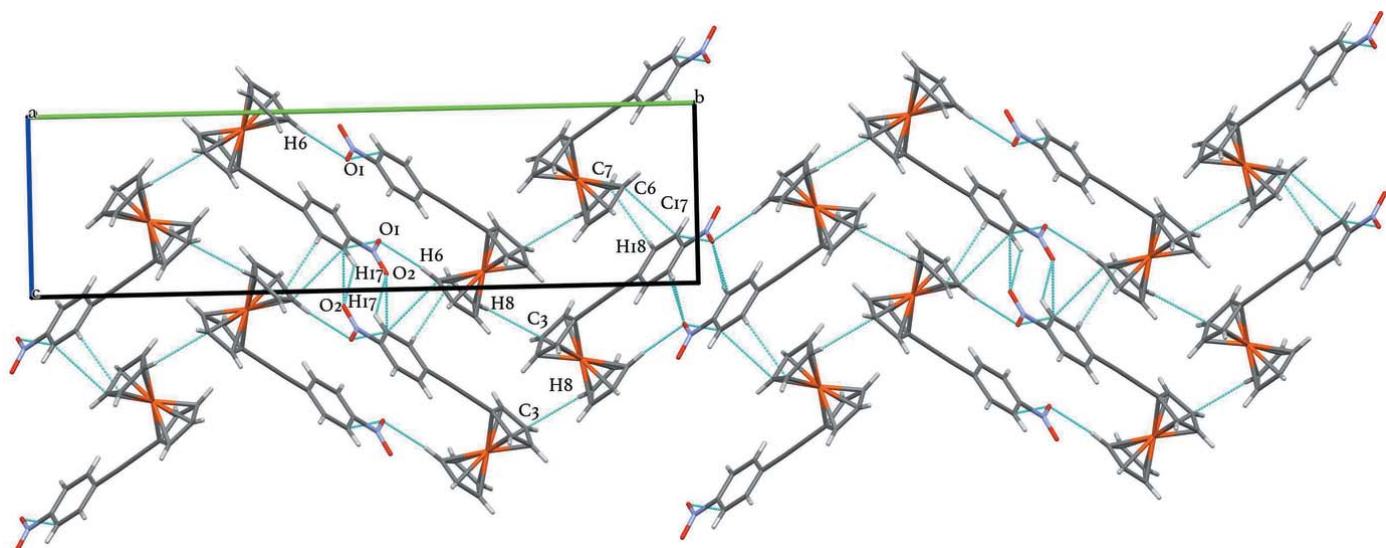

Figure 2
Crystal packing of the title compound along the *a* axis with short-contact interactions shown as dashed lines.
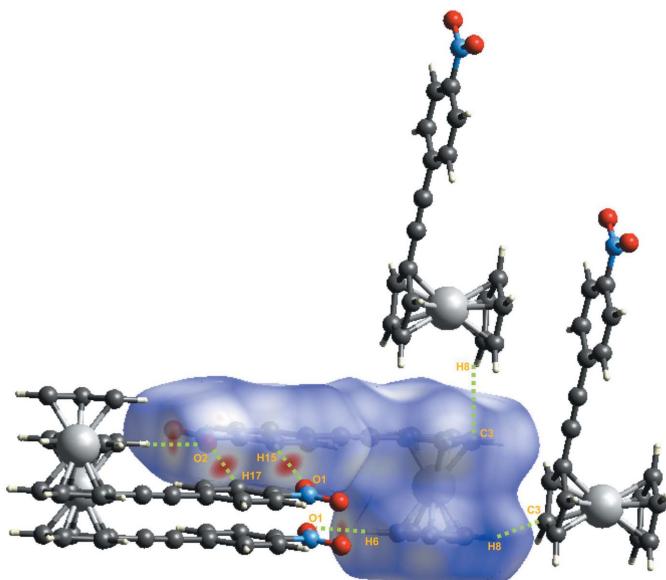
Figure 3
A view of the Hirshfeld surface of the title compound mapped over d_{norm} with the four main intermolecular contacts in the crystal lattice.

yl)$\cdots$O2(*p*-nitrophenyl) with a distance of 2.727 (2) Å and pairs from O1(*p*-nitrophenyl)$\cdots$H15—C15(*p*-nitrophenyl) with a distance of 2.716 (2) Å. In addition, a chain is formed by short contacts from the C17—H17(*p*-nitrophenyl)$\cdots$O1(*p*-nitrophenyl) interaction belonging to the *p*-nitrophenyl substituent with a distance of 3.203 (19) Å. Numerical details of the hydrogen-bonding interactions are given in Table 1 and the packing is shown in Fig. 2.

4. Hirshfeld Surface Analysis

CrystalExplorer17 (Turner *et al.*, 2017) was used to generate the Hirshfeld surface (Spackman & Jayatilaka, 2009) for the title compound mapped over d_{norm} and the associated two-dimensional fingerprint plots (McKinnon *et al.*, 2007). Fig. 3 shows the molecules involved in the four closest contacts. Red
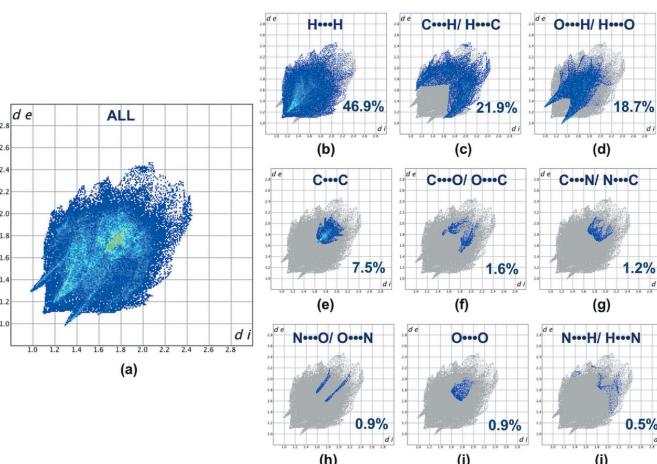

Figure 4
Full (*a*) and individual (*b*)–(*j*) two-dimensional fingerprint plots showing the nine intermolecular contacts present in the crystal structure.

Table 2
The effect of the substituent on the dihedral angle (°) between the substituted Cp ring and the phenyl ring in compounds containing a 1-ferrocenyl-2-phenylethyne backbone and a *para*-substituted phenyl ring.

Substituent	Dihedral angle	Refcode
Methyl (CH$_3$)	1.01 (9)	YOHSIY (Bobula *et al.*, 2008)
Nitro (NO$_2$)	6.61 (9)	This work
Amino (NH$_2$)	8.05 (9)	YONFEN (Siemeling *et al.*, 2008)
Ethynyl (C≡CH)	8.61 (9)	RARNED (Lin *et al.*, 1996)
Iodo (I)	37.25 (9)	GIZTOA (Misra *et al.*, 2014)
Cyano (C≡N)	69.58 (9)	MIJLAS01 (Bobula *et al.*, 2008)
Hydrogen (H)	89.06 (9)	KELTIF (Zora *et al.*, 2006)
Trifluoromethyl (CF$_3$)	90.00 (9)	YOKSUK01 (Dai *et al.*, 2013)

spots on the Hirshfeld surface mapped over d_{norm} in the color range −0.2315 to 1.1417 arbitrary units confirm the previously mentioned main intermolecular contacts. The fingerprint plots are given for all contacts (Fig. 4*a*) and those decomposed into nine individual interactions: H$\cdots$H (46.9%; Fig. 4*b*), C$\cdots$H/ H$\cdots$C (21.9%; Fig. 4*c*), O$\cdots$H/ H$\cdots$O (18.7%; Fig. 4*d*), C$\cdots$C (7.5%; Fig. 4*e*), C$\cdots$O/O$\cdots$C (1.6%; Fig. 4*f*), C$\cdots$N/N$\cdots$C (1.2%; Fig. 4*g*), N$\cdots$O/O$\cdots$N (0.9%; Fig. 4*h*), O$\cdots$O (0.9%; Fig. 4*i*) and N$\cdots$H/H$\cdots$N (0.5%; Fig. 4*j*). The Hirshfeld surface analysis for the title compound indicates that the most significant contributions arise from H$\cdots$H and C$\cdots$H contacts (González *et al.*, 2020; McKinnon *et al.*, 2004, 2007; Spackman & McKinnon, 2002).

5. Database survey

A search of the Cambridge Structural Database (Version 5.41, updated November 2019; Groom *et al.*, 2016) revealed 142 related compounds with the 1-ferrocenyl-2-phenylethyne backbone. Of those structures, 41 contain substituents in the *para* position of the phenyl ring, as in the title compound. One of the reasons for such a high number of reported structures for methynylferrocene and its derived compounds is attributed to their substantial interest as chromophores, mainly because of their electronic communication capacity through the alkyne linkage to the Fe center. When comparing the effect of the substituent on the molecular structure, one of the main features is the dihedral angle that is formed between the substituted Cp ring of the ferrocene group and the phenyl moiety. The orientation can range from almost parallel (1.01°: YOHSIY; Bobula *et al.*, 2008) to completely perpendicular (90.00°: YOHSUK01; Dai *et al.*, 2013). Table 2 gives the dihedral angles for previously reported compounds; our compound having the second lowest dihedral angle and a nearly parallel conformation. Exchanging the hydrogen atoms in the methyl group for fluorine atoms shifts the dihedral angle from 1.01° to 90.00° in the case of methyl and trifluoromethyl substituents, respectively.

6. Synthesis and crystallization

The title compound was prepared by adding ethynylferrocene (1.0 mmol), PdCl$_2$(PPh$_3$)$_2$ (0.01 mmol), Et$_3$N (2 mmol) and 4-bromo-1-nitrobenzene (1.0 mmol) to a 25 mL round-bottom

flask, followed by the addition of DMF (1.0 mL) by syringe. The reaction was stirred for 1 h at 353 K. The reaction was stopped and crashed out with 20 mL of cold distilled water, then the solid was vacuum filtrated, and chromatographed [silica (heptane–ethyl acetate/7:3)] to afford the pure compound, 70% yield. Dark-red crystals suitable for X-ray diffraction were obtained by the slow evaporation of $CDCl_3$ solution of the title compound at room temperature. NMR analyses were performed on a Bruker AV-700 spectrometer by using $CDCl_3$ 99.9% pure as a solvent and Me_4Si as external standard. ^{1}H NMR (δ in ppm, $CDCl_3$): 4.26 (s, 5H), 4.32 (s, 2H), 4.55 (s, 2H), 7.59 (d, J = 8.6Hz, 2H), 8.18 (d, J = 8.6Hz, 2H). ^{13}C NMR (δ in ppm, $CDCl_3$): 63.6, 69.6, 70.1, 71.8, 84.5, 95.2, 123.6, 131.1, 131.8, 146.4. IR (ν_{max}, cm^{-1}): 2200 (C≡C). Electrochemistry: ($CV_{200\ mv}$: E^o = 613 mV; ΔE = 90 mV).

7. Refinement

Crystal data, data collection and structure refinement details are summarized in Table 3. H atoms were included in geometrically calculated positions, C—H = 0.93 Å, and refined as riding on their parent C atom with $U_{iso}(H) = 1.2U_{eq}(C)$.

References

Bobula, T., Hudlický, J., Novák, P., Gyepes, R., Císařová, I., Štěpnička, P. & Kotora, M. (2008). *Eur. J. Inorg. Chem.* pp. 3911–3920.

Coutouli-Argyropoulou, E., Tsitabani, M., Petrantonakis, G., Terzis, A. & Raptopoulou, C. (2003). *Org. Biomol. Chem.* **1**, 1382–1388.

Dai, J.-J., Fang, C., Xiao, B., Yi, J., Xu, J., Liu, Z.-J., Lu, X., Liu, L. & Fu, Y. (2013). *J. Am. Chem. Soc.* **135**, 8436–8439.

Dolomanov, O. V., Bourhis, L. J., Gildea, R. J., Howard, J. A. K. & Puschmann, H. (2009). *J. Appl. Cryst.* **42**, 339–341.

Fu, N., Zhang, Y., Yang, D., Chen, B. & Wu, X. (2008). *Catal. Commun.* **9**, 976–979.

Gasser, G. & Metzler-Nolte, N. (2012). *Curr. Opin. Chem. Biol.* **16**, 84–91.

González Espiet, J. C., Cintrón Cruz, J. A. & Piñero Cruz, D. M. (2020). *Acta Cryst.* E**76**, 231–234.

Görmen, M., Pigeon, P., Hillard, E., Vessières, A., Huché, M., Richard, M., McGlinchey, M., Top, S. & Jaouen, G. (2012). *Organometallics*, **31**, 5856–5866.

Groom, C. R., Bruno, I. J., Lightfoot, M. P. & Ward, S. C. (2016). *Acta Cryst.* B**72**, 171–179.

Kulhánek, J., Bureš, F., Opršal, J., Kuznik, W., Mikysek, T. & Růžička, A. (2013). *Asia. J. Org. Chem.* **2**, 422–431.

Li, C., Zhang, C., Zhang, W., Zhu, Q., Cheng, H. & Chen, B. (2009). *Catal. Commun.* **10**, 1006–1009.

Lin, J. T., Wu, J. J., Li, C., Wen, Y. S. & Lin, K. (1996). *Organometallics*, **15**, 5028–5034.

Macrae, C. F., Sovago, I., Cottrell, S. J., Galek, P. T. A., McCabe, P., Pidcock, E., Platings, M., Shields, G. P., Stevens, J. S., Towler, M. & Wood, P. A. (2020). *J. Appl. Cryst.* **53**, 226–235.

McKinnon, J. J., Jayatilaka, D. & Spackman, M. A. (2007). *Chem. Commun.* 3814–3816.

McKinnon, J. J., Spackman, M. A. & Mitchell, A. S. (2004). *Acta Cryst.* B**60**, 627–668.

Misra, R., Maragani, R., Jadhav, T. & Mobin, S. M. (2014). *New J. Chem.* **38**, 1446–1450.

Rigaku OD (2018). *CrysAlis PRO*. Rigaku Oxford Diffraction, Yarnton, England.

Sheldrick, G. M. (2015a). *Acta Cryst.* A**71**, 3–8.

Sheldrick, G. M. (2015b). *Acta Cryst.* C**71**, 3–8.

Shoji, T., Maruyama, A., Yaku, C., Kamata, N., Ito, S., Okujima, T. & Toyota, K. (2014). *Chem. Eur. J.* **20**, 1–9.

Siemeling, U., Bruhn, C., Meier, M. & Schirrmacher, C. (2008). *Z. Naturforsch. B: Chem. Sci.* **63**, 1395–1401.

Spackman, M. A. & Jayatilaka, D. (2009). *CrystEngComm*, **11**, 19–32.

Spackman, M. A. & McKinnon, J. J. (2002). *CrystEngComm*, **4**, 378–392.

Torres, J. C., Pilli, R. A., Vargas, M. D., Violante, F. A., Garden, S. J. & Pinto, A. C. (2002). *Tetrahedron*, **58**, 4487–4492.

Turner, M. J., Mckinnon, J. J., Wolff, S. K., Grimwood, D. J., Spackman, P. R., Jayatilaka, D. & Spackman, M. A. (2017). *CrystalExplorer17*. The University of Western Australia.

Zora, M., Açıkgöz, C., Tumay, T. A., Odabaşoğlu, M. & Büyükgüngör, O. (2006). *Acta Cryst.* C**62**, m327–m330.

Table 3
Experimental details.

Crystal data	
Chemical formula	$[Fe(C_5H_5)_2(C_8NO_2)]$
M_r	331.14
Crystal system, space group	Monoclinic, $P2_1/n$
Temperature (K)	100
a, b, c (Å)	5.9573 (1), 29.3810 (3), 8.0664 (1)
β (°)	100.202 (1)
V (Å^3)	1389.55 (3)
Z	4
Radiation type	Cu $K\alpha$
μ (mm^{-1})	8.75
Crystal size (mm)	$0.20 \times 0.07 \times 0.04$
Data collection	
Diffractometer	Rigaku SuperNova, Single source at offset/far, HyPix3000
Absorption correction	Multi-scan (*CrysAlis PRO*; Rigaku OD, 2018)
T_{min}, T_{max}	0.642, 1.000
No. of measured, independent and observed [$I > 2\sigma(I)$] reflections	21951, 2567, 2410
R_{int}	0.036
$(\sin\theta/\lambda)_{max}$ (Å^{-1})	0.605
Refinement	
$R[F^2 > 2\sigma(F^2)]$, $wR(F^2)$, S	0.024, 0.061, 1.07
No. of reflections	2567
No. of parameters	200
H-atom treatment	H-atom parameters constrained
$\Delta\rho_{max}$, $\Delta\rho_{min}$ (e Å^{-3})	0.23, −0.37

Computer programs: *CrysAlis PRO* (Rigaku OD, 2018), *SHELXT* (Sheldrick, 2015a), *SHELXL* (Sheldrick, 2015b) and *OLEX2* (Dolomanov et al., 2009).

supporting information

Crystal structure of 1-ferrocenyl-2-(4-nitrophenyl)ethyne

Sara M. Delgado Rivera, Jean C. González Espiet, Jesús M. Dones, Sebastián A. Henríquez López, Ana R. Guadalupe, Dalice M. Piñero Cruz and Ingrid Montes González

Computing details

Data collection: *CrysAlis PRO* (Rigaku OD, 2018); cell refinement: *CrysAlis PRO* (Rigaku OD, 2018); data reduction: *CrysAlis PRO* (Rigaku OD, 2018); program(s) used to solve structure: ShelXT (Sheldrick, 2015a); program(s) used to refine structure: *SHELXL* (Sheldrick, 2015b); molecular graphics: *OLEX2* (Dolomanov *et al.*, 2009); software used to prepare material for publication: *OLEX2* (Dolomanov *et al.*, 2009).

1-Ferrocenyl-2-(4-nitrophenyl)ethyne

Crystal data

$[Fe(C_5H_5)_2(C_8NO_2)]$	$F(000) = 680$
$M_r = 331.14$	$D_x = 1.583$ Mg m^{-3}
Monoclinic, $P2_1/n$	Cu $K\alpha$ radiation, $\lambda = 1.54184$ Å
$a = 5.9573$ (1) Å	Cell parameters from 12369 reflections
$b = 29.3810$ (3) Å	$\theta = 3.0–68.8°$
$c = 8.0664$ (1) Å	$\mu = 8.75$ mm^{-1}
$\beta = 100.202$ (1)°	$T = 100$ K
$V = 1389.55$ (3) Å^3	Block, dark red
$Z = 4$	$0.20 \times 0.07 \times 0.04$ mm

Data collection

Rigaku SuperNova, Single source at offset/far, HyPix3000 diffractometer	$T_{min} = 0.642$, $T_{max} = 1.000$
	21951 measured reflections
	2567 independent reflections
Radiation source: micro-focus sealed X-ray tube, SuperNova (Cu) X-ray Source	2410 reflections with $I > 2\sigma(I)$
	$R_{int} = 0.036$
Mirror monochromator	$\theta_{max} = 68.9°$, $\theta_{min} = 3.0°$
ω scans	$h = -7 \rightarrow 7$
Absorption correction: multi-scan (CrysAlisPro; Rigaku OD, 2018)	$k = -35 \rightarrow 35$
	$l = -9 \rightarrow 9$

Refinement

Refinement on F^2	Hydrogen site location: inferred from neighbouring sites
Least-squares matrix: full	H-atom parameters constrained
$R[F^2 > 2\sigma(F^2)] = 0.024$	$w = 1/[\sigma^2(F_o^2) + (0.0305P)^2 + 0.6401P]$ where $P = (F_o^2 + 2F_c^2)/3$
$wR(F^2) = 0.061$	
$S = 1.07$	$(\Delta/\sigma)_{max} = 0.003$
2567 reflections	$\Delta\rho_{max} = 0.23$ e Å^{-3}
200 parameters	$\Delta\rho_{min} = -0.37$ e Å^{-3}
0 restraints	
Primary atom site location: dual	

Extinction correction: SHELXL-2018/3
(Sheldrick 2015b),
$Fc^*=kFc[1+0.001xFc^2\lambda^3/\sin(2\theta)]^{-1/4}$
Extinction coefficient: 0.00060 (13)

Special details

Geometry. All esds (except the esd in the dihedral angle between two l.s. planes) are estimated using the full covariance matrix. The cell esds are taken into account individually in the estimation of esds in distances, angles and torsion angles; correlations between esds in cell parameters are only used when they are defined by crystal symmetry. An approximate (isotropic) treatment of cell esds is used for estimating esds involving l.s. planes.

Fractional atomic coordinates and isotropic or equivalent isotropic displacement parameters ($Å^2$)

	x	*y*	*z*	U_{iso}*/U_{eq}
Fe1	0.76257 (4)	0.67811 (2)	0.90888 (3)	0.01397 (9)
O1	−0.49667 (19)	0.47779 (4)	0.27187 (15)	0.0226 (3)
O2	−0.2775 (2)	0.46760 (4)	0.08806 (15)	0.0271 (3)
N1	−0.3245 (2)	0.48668 (4)	0.21343 (17)	0.0167 (3)
C1	0.5321 (3)	0.68695 (5)	0.6915 (2)	0.0173 (3)
C2	0.7551 (3)	0.70112 (5)	0.6686 (2)	0.0192 (3)
H2	0.837507	0.689297	0.590834	0.023*
C3	0.8274 (3)	0.73649 (5)	0.7863 (2)	0.0208 (3)
H3	0.965574	0.751951	0.798205	0.025*
C4	0.6531 (3)	0.74426 (5)	0.8827 (2)	0.0205 (3)
H4	0.657556	0.765623	0.968280	0.025*
C5	0.4711 (3)	0.71379 (5)	0.8256 (2)	0.0198 (3)
H5	0.335922	0.711567	0.867718	0.024*
C6	0.7951 (3)	0.60950 (5)	0.9567 (2)	0.0221 (4)
H6	0.732434	0.586180	0.885223	0.026*
C7	1.0133 (3)	0.62957 (5)	0.9617 (2)	0.0193 (3)
H7	1.118391	0.621784	0.893815	0.023*
C8	1.0425 (3)	0.66366 (5)	1.0887 (2)	0.0192 (3)
H8	1.170282	0.682060	1.118684	0.023*
C9	0.8431 (3)	0.66474 (6)	1.1617 (2)	0.0212 (4)
H9	0.817060	0.683939	1.247992	0.025*
C10	0.6897 (3)	0.63126 (6)	1.0798 (2)	0.0233 (4)
H10	0.545564	0.624788	1.103002	0.028*
C11	0.3932 (3)	0.65207 (5)	0.6029 (2)	0.0189 (3)
C12	0.2680 (3)	0.62353 (6)	0.5308 (2)	0.0195 (3)
C13	0.1182 (3)	0.58890 (5)	0.4500 (2)	0.0170 (3)
C14	−0.0833 (3)	0.57845 (5)	0.5091 (2)	0.0182 (3)
H14	−0.119391	0.594223	0.600861	0.022*
C15	−0.2291 (3)	0.54491 (5)	0.43247 (19)	0.0167 (3)
H15	−0.363101	0.537993	0.471276	0.020*
C16	−0.1700 (3)	0.52188 (5)	0.2961 (2)	0.0153 (3)
C17	0.0281 (3)	0.53113 (5)	0.2348 (2)	0.0170 (3)
H17	0.063821	0.515003	0.143683	0.020*
C18	0.1713 (3)	0.56480 (5)	0.3118 (2)	0.0182 (3)
H18	0.304440	0.571598	0.271639	0.022*

Atomic displacement parameters (Å²)

	U^{11}	U^{22}	U^{33}	U^{12}	U^{13}	U^{23}
Fe1	0.01496 (14)	0.01010 (14)	0.01622 (15)	−0.00021 (9)	0.00100 (10)	0.00119 (9)
O1	0.0200 (6)	0.0236 (6)	0.0264 (6)	−0.0064 (5)	0.0101 (5)	−0.0040 (5)
O2	0.0305 (7)	0.0265 (7)	0.0274 (7)	−0.0059 (5)	0.0137 (6)	−0.0127 (5)
N1	0.0188 (7)	0.0139 (6)	0.0179 (7)	0.0005 (5)	0.0049 (5)	0.0000 (5)
C1	0.0184 (8)	0.0138 (7)	0.0183 (8)	0.0005 (6)	−0.0004 (7)	0.0045 (6)
C2	0.0213 (8)	0.0158 (8)	0.0207 (8)	−0.0001 (6)	0.0039 (7)	0.0054 (6)
C3	0.0187 (8)	0.0142 (8)	0.0278 (9)	−0.0020 (6)	−0.0008 (7)	0.0071 (7)
C4	0.0233 (9)	0.0117 (7)	0.0243 (9)	0.0027 (6)	−0.0015 (7)	0.0004 (6)
C5	0.0180 (8)	0.0163 (8)	0.0244 (9)	0.0023 (6)	0.0020 (7)	0.0025 (6)
C6	0.0282 (9)	0.0111 (8)	0.0236 (9)	−0.0010 (6)	−0.0047 (7)	0.0037 (6)
C7	0.0216 (8)	0.0149 (8)	0.0205 (8)	0.0050 (6)	0.0011 (7)	0.0021 (6)
C8	0.0201 (8)	0.0151 (8)	0.0201 (8)	−0.0003 (6)	−0.0024 (7)	0.0021 (6)
C9	0.0274 (9)	0.0200 (8)	0.0161 (8)	0.0035 (7)	0.0030 (7)	0.0022 (6)
C10	0.0203 (8)	0.0229 (9)	0.0262 (9)	−0.0016 (7)	0.0026 (7)	0.0106 (7)
C11	0.0200 (8)	0.0165 (8)	0.0196 (8)	0.0012 (6)	0.0014 (7)	0.0032 (6)
C12	0.0203 (8)	0.0177 (8)	0.0200 (8)	0.0017 (7)	0.0026 (7)	0.0037 (7)
C13	0.0190 (8)	0.0131 (7)	0.0176 (8)	0.0007 (6)	−0.0005 (6)	0.0041 (6)
C14	0.0225 (8)	0.0166 (8)	0.0155 (8)	0.0018 (6)	0.0032 (6)	−0.0001 (6)
C15	0.0176 (8)	0.0164 (8)	0.0165 (8)	0.0010 (6)	0.0045 (6)	0.0022 (6)
C16	0.0175 (8)	0.0123 (7)	0.0159 (8)	−0.0002 (6)	0.0019 (6)	0.0011 (6)
C17	0.0183 (8)	0.0162 (8)	0.0169 (8)	0.0023 (6)	0.0048 (6)	0.0006 (6)
C18	0.0172 (8)	0.0177 (8)	0.0200 (8)	0.0007 (6)	0.0038 (6)	0.0045 (6)

Geometric parameters (Å, º)

Fe1—C1	2.0431 (17)	C6—H6	0.9300
Fe1—C2	2.0454 (16)	C6—C7	1.422 (2)
Fe1—C3	2.0505 (16)	C6—C10	1.418 (3)
Fe1—C4	2.0491 (16)	C7—H7	0.9300
Fe1—C5	2.0375 (16)	C7—C8	1.421 (2)
Fe1—C6	2.0552 (16)	C8—H8	0.9300
Fe1—C7	2.0546 (16)	C8—C9	1.417 (2)
Fe1—C8	2.0515 (17)	C9—H9	0.9300
Fe1—C9	2.0489 (17)	C9—C10	1.423 (3)
Fe1—C10	2.0488 (16)	C10—H10	0.9300
O1—N1	1.2301 (17)	C11—C12	1.202 (2)
O2—N1	1.2312 (17)	C12—C13	1.432 (2)
N1—C16	1.464 (2)	C13—C14	1.402 (2)
C1—C2	1.435 (2)	C13—C18	1.403 (2)
C1—C5	1.437 (2)	C14—H14	0.9300
C1—C11	1.427 (2)	C14—C15	1.385 (2)
C2—H2	0.9300	C15—H15	0.9300
C2—C3	1.422 (2)	C15—C16	1.389 (2)
C3—H3	0.9300	C16—C17	1.385 (2)
C3—C4	1.422 (2)	C17—H17	0.9300

C4—H4	0.9300	C17—C18	1.380 (2)
C4—C5	1.418 (2)	C18—H18	0.9300
C5—H5	0.9300		

C1—Fe1—C2	41.09 (6)	C4—C3—C2	108.54 (14)
C1—Fe1—C3	68.60 (6)	C4—C3—H3	125.7
C1—Fe1—C4	68.76 (6)	Fe1—C4—H4	126.6
C1—Fe1—C6	108.20 (7)	C3—C4—Fe1	69.76 (9)
C1—Fe1—C7	128.28 (7)	C3—C4—H4	125.9
C1—Fe1—C8	166.33 (7)	C5—C4—Fe1	69.25 (9)
C1—Fe1—C9	151.89 (7)	C5—C4—C3	108.16 (15)
C1—Fe1—C10	118.21 (7)	C5—C4—H4	125.9
C2—Fe1—C3	40.62 (7)	Fe1—C5—H5	125.9
C2—Fe1—C4	68.63 (7)	C1—C5—Fe1	69.60 (9)
C2—Fe1—C6	119.18 (7)	C1—C5—H5	126.0
C2—Fe1—C7	108.59 (7)	C4—C5—Fe1	70.13 (9)
C2—Fe1—C8	128.09 (7)	C4—C5—C1	108.06 (15)
C2—Fe1—C9	165.58 (7)	C4—C5—H5	126.0
C2—Fe1—C10	152.64 (7)	Fe1—C6—H6	126.3
C3—Fe1—C6	153.07 (7)	C7—C6—Fe1	69.74 (9)
C3—Fe1—C7	119.24 (7)	C7—C6—H6	126.0
C3—Fe1—C8	108.37 (7)	C10—C6—Fe1	69.55 (9)
C4—Fe1—C3	40.58 (7)	C10—C6—H6	126.0
C4—Fe1—C6	165.33 (7)	C10—C6—C7	108.03 (15)
C4—Fe1—C7	152.40 (7)	Fe1—C7—H7	126.1
C4—Fe1—C8	118.25 (7)	C6—C7—Fe1	69.78 (9)
C5—Fe1—C1	41.23 (7)	C6—C7—H7	126.1
C5—Fe1—C2	69.11 (7)	C8—C7—Fe1	69.63 (9)
C5—Fe1—C3	68.47 (7)	C8—C7—C6	107.88 (15)
C5—Fe1—C4	40.62 (7)	C8—C7—H7	126.1
C5—Fe1—C6	127.80 (7)	Fe1—C8—H8	126.1
C5—Fe1—C7	166.23 (7)	C7—C8—Fe1	69.87 (9)
C5—Fe1—C8	151.41 (7)	C7—C8—H8	125.9
C5—Fe1—C9	117.54 (7)	C9—C8—Fe1	69.69 (9)
C5—Fe1—C10	107.31 (7)	C9—C8—C7	108.12 (15)
C7—Fe1—C6	40.48 (7)	C9—C8—H8	125.9
C8—Fe1—C6	68.07 (7)	Fe1—C9—H9	126.0
C8—Fe1—C7	40.50 (6)	C8—C9—Fe1	69.89 (9)
C9—Fe1—C3	127.56 (7)	C8—C9—H9	126.0
C9—Fe1—C4	107.38 (7)	C8—C9—C10	107.97 (15)
C9—Fe1—C6	68.12 (7)	C10—C9—Fe1	69.67 (9)
C9—Fe1—C7	68.10 (7)	C10—C9—H9	126.0
C9—Fe1—C8	40.42 (7)	Fe1—C10—H10	125.9
C10—Fe1—C3	165.28 (7)	C6—C10—Fe1	70.03 (9)
C10—Fe1—C4	127.24 (7)	C6—C10—C9	108.00 (15)
C10—Fe1—C6	40.42 (7)	C6—C10—H10	126.0
C10—Fe1—C7	68.11 (7)	C9—C10—Fe1	69.68 (9)
C10—Fe1—C8	68.14 (7)	C9—C10—H10	126.0

C10—Fe1—C9	40.65 (7)	C12—C11—C1	177.07 (18)
O1—N1—O2	123.00 (13)	C11—C12—C13	178.15 (18)
O1—N1—C16	118.36 (13)	C14—C13—C12	120.19 (15)
O2—N1—C16	118.63 (13)	C14—C13—C18	119.13 (15)
C2—C1—Fe1	69.54 (9)	C18—C13—C12	120.67 (15)
C2—C1—C5	107.51 (14)	C13—C14—H14	119.6
C5—C1—Fe1	69.18 (9)	C15—C14—C13	120.74 (15)
C11—C1—Fe1	125.49 (11)	C15—C14—H14	119.6
C11—C1—C2	127.74 (15)	C14—C15—H15	120.9
C11—C1—C5	124.74 (15)	C14—C15—C16	118.24 (14)
Fe1—C2—H2	126.2	C16—C15—H15	120.9
C1—C2—Fe1	69.37 (9)	C15—C16—N1	118.51 (14)
C1—C2—H2	126.1	C17—C16—N1	118.86 (14)
C3—C2—Fe1	69.88 (9)	C17—C16—C15	122.62 (15)
C3—C2—C1	107.72 (14)	C16—C17—H17	120.7
C3—C2—H2	126.1	C18—C17—C16	118.53 (15)
Fe1—C3—H3	126.7	C18—C17—H17	120.7
C2—C3—Fe1	69.50 (9)	C13—C18—H18	119.6
C2—C3—H3	125.7	C17—C18—C13	120.73 (15)
C4—C3—Fe1	69.66 (9)	C17—C18—H18	119.6
Fe1—C1—C2—C3	−59.59 (11)	C5—C1—C2—C3	−0.63 (18)
Fe1—C1—C5—C4	59.82 (11)	C6—C7—C8—Fe1	−59.53 (11)
Fe1—C2—C3—C4	−58.88 (11)	C6—C7—C8—C9	−0.12 (18)
Fe1—C3—C4—C5	−58.78 (11)	C7—C6—C10—Fe1	59.33 (11)
Fe1—C4—C5—C1	−59.48 (11)	C7—C6—C10—C9	−0.24 (18)
Fe1—C6—C7—C8	59.43 (11)	C7—C8—C9—Fe1	−59.51 (11)
Fe1—C6—C10—C9	−59.57 (12)	C7—C8—C9—C10	−0.02 (18)
Fe1—C7—C8—C9	59.40 (11)	C8—C9—C10—Fe1	−59.63 (11)
Fe1—C8—C9—C10	59.49 (11)	C8—C9—C10—C6	0.16 (19)
Fe1—C9—C10—C6	59.79 (11)	C10—C6—C7—Fe1	−59.21 (11)
O1—N1—C16—C15	−2.5 (2)	C10—C6—C7—C8	0.22 (18)
O1—N1—C16—C17	177.91 (14)	C11—C1—C2—Fe1	−119.65 (17)
O2—N1—C16—C15	176.88 (14)	C11—C1—C2—C3	−179.24 (15)
O2—N1—C16—C17	−2.7 (2)	C11—C1—C5—Fe1	119.48 (16)
N1—C16—C17—C18	179.07 (14)	C11—C1—C5—C4	179.29 (15)
C1—C2—C3—Fe1	59.27 (11)	C12—C13—C14—C15	−179.76 (15)
C1—C2—C3—C4	0.39 (18)	C12—C13—C18—C17	179.41 (15)
C2—C1—C5—Fe1	−59.19 (11)	C13—C14—C15—C16	0.2 (2)
C2—C1—C5—C4	0.62 (18)	C14—C13—C18—C17	−0.2 (2)
C2—C3—C4—Fe1	58.78 (11)	C14—C15—C16—N1	−179.41 (14)
C2—C3—C4—C5	−0.01 (18)	C14—C15—C16—C17	0.1 (2)
C3—C4—C5—Fe1	59.10 (11)	C15—C16—C17—C18	−0.4 (2)
C3—C4—C5—C1	−0.38 (18)	C16—C17—C18—C13	0.5 (2)
C5—C1—C2—Fe1	58.96 (11)	C18—C13—C14—C15	−0.2 (2)

Hydrogen-bond geometry (Å, º)

D—H···A	D—H	H···A	D···A	D—H···A
C6—H6···O1[i]	0.93	2.55	3.461 (2)	168
C15—H15···O1[ii]	0.93	2.41	3.1909 (19)	141
C17—H17···O2[iii]	0.93	2.49	3.2187 (19)	135

Symmetry codes: (i) −*x*, −*y*+1, −*z*+1; (ii) −*x*−1, −*y*+1, −*z*+1; (iii) −*x*, −*y*+1, −*z*.